# Working Memory Load-related Theta Power Decreases in Dorsolateral Prefrontal Cortex Predict Individual Differences in Performance

**Aneta Brzezicka[1,2], Jan Kamiński[1,3], Chrystal M. Reed[1], Jeffrey M. Chung[1], Adam N. Mamelak[1], and Ueli Rutishauser[1,3]**

## Abstract

■ Holding information in working memory (WM) is an active and effortful process that is accompanied by sustained load-dependent changes in oscillatory brain activity. These proportional power increases are often reported in EEG studies recording theta over frontal midline sites. Intracranial recordings, however, yield mixed results, depending on the brain area being recorded from. We recorded intracranial EEG with depth electrodes in 13 patients with epilepsy who were performing a Sternberg WM task. Here, we investigated patterns of theta power changes as a function of memory load during maintenance in three areas critical for WM: dorsolateral prefrontal cortex (DLPFC), dorsal ACC (dACC), and hippocampus. Theta frequency power in both hippocampus and dACC increased during maintenance. In contrast, theta frequency power in the DLPFC decreased during maintenance, and this decrease was proportional to memory load. Only the power decreases in DLPFC, but not the power increases in hippocampus and dACC, were predictive of behavior in a given trial. The extent of the load-related theta power decreases in the DLPFC in a given participant predicted a participant's RTs, revealing that DLPFC theta explains individual differences in WM ability between participants. Together, these data reveal a pattern of theta power decreases in the DLPFC that is predictive of behavior and that is opposite of that in other brain areas. This result suggests that theta band power changes serve different cognitive functions in different brain areas and specifically that theta power decreases in DLPFC have an important role in maintenance of information. ■

## INTRODUCTION

Maintaining information in the absence of external stimuli is crucial for many cognitive functions (Unsworth & Engle, 2006, 2007). The ability to actively hold a piece of information in mind and resist interference forms the core of the working memory (WM) system (Baddeley, 2010). The capacity of an individual's WM is predictive of that person's cognitive ability in a number of domains, including analytic problem solving (Wiley & Jarosz, 2012), reading (Nouwens, Groen, & Verhoeven, 2017), and fluid intelligence (Shipstead, Harrison, & Engle, 2016)—a finding that highlights the broad importance of WM for someone's overall cognitive abilities.

Holding information in WM is an active and effortful task that is thought to depend on the large-scale interaction of multiple brain areas. This interaction is thought to be coordinated by synchronized oscillations—a view supported by the finding that the maintenance of information in WM leads to substantial changes in the oscillatory activity of field potentials in many brain areas. Theta frequency (3–8 Hz) band power increases are among the most consistently documented during WM maintenance. This increase was found in many areas, including medial prefrontal cortex (pFC), the hippocampus (Maurer et al., 2015; Axmacher et al., 2010; Tsujimoto, Shimazu, Isomura, & Sasaki, 2010; Onton, Delorme, & Makeig, 2005; Tesche & Karhu, 2000), and sensory areas (Lee, Simpson, Logothetis, & Rainer, 2005). The magnitude of this increase in theta power is typically proportional to the amount of the information being held in mind, with higher loads and/or higher effort resulting in higher theta band power (Gärtner, Grimm, & Bajbouj, 2015; Maurer et al., 2015; Wisniewski et al., 2015; Meltzer et al., 2008; Howard et al., 2003; Jensen & Tesche, 2002). Also, theta band power changes are predictive of behaviors that depend on WM (Zakrzewska & Brzezicka, 2014; Lega, Jacobs, & Kahana, 2012; Womelsdorf, Johnston, Vinck, & Everling, 2010)—a result that shows that theta band activity is functionally relevant for this kind of cognitive activity.

An extensive body of literature indicates that medial frontal cortex (MFC), dorsolateral prefrontal cortex (DLPFC), and the hippocampus serve important roles in WM maintenance. However, the distinct roles of each

This paper is part of a Special Focus deriving from a symposium at the 2018 Annual Meeting of the Cognitive Neuroscience Society entitled "Episodic Memory Formation: From Neural Circuits to Behavior."

[1]Cedars-Sinai Medical Center, Los Angeles, CA, [2]SWPS University of Social Sciences and Humanities, Warsaw, Poland, [3]California Institute of Technology

in WM is poorly understood. Although extensively observed in scalp EEG studies (Roux & Uhlhaas, 2014; Meltzer, Negishi, Mayes, & Constable, 2007) and specifically for frontal midline theta (FMT; Gärtner et al., 2015; Maurer et al., 2015; Mitchell, McNaughton, Flanagan, & Kirk, 2008; Onton et al., 2005; Asada, Fukuda, Tsunoda, Yamaguchi, & Tonoike, 1999), it remains unclear which brain areas specifically contribute to the observed theta power increases in scalp EEG. Because each EEG electrode is sensitive to electrical fields generated by large populations of neurons that may be spatially distributed, there is not necessarily a one-to-one mapping between scalp electrode location and the source of the underlying neural activity. Consequently, the scalp FMT power changes are likely a mixture of activity in many areas, including the hippocampus.

To better differentiate the distinct contributions of different areas to WM, direct intracranial recordings are crucial. Here, we simultaneously record from all three areas using intracranial recordings in epilepsy patients implanted with depth electrodes. We then characterize and compare the properties of theta during WM maintenance in each region. The principle goal of this study is twofold: first, to determine whether medial frontal (dorsal part of the ACC, dACC), lateral prefrontal (DLPFC), and medial temporal (hippocampus) areas show similar or differential patterns of changes in theta power during WM maintenance and, second, to quantify which of these theta-changes predicts behavior.

Of particular interest in this study is the DLPFC, which is thought to be a key structure in coordinating—via oscillatory dynamics—large-scale neuronal interactions in a task-depended manner (Helfrich & Knight, 2016). Oscillatory mechanisms underlying cognitive processes were first described in the hippocampus and primary sensory areas of rodents and nonhuman primates, but recent work suggests that higher cognitive processes, including WM, are also facilitated by similar oscillatory mechanisms (Helfrich & Knight, 2016; Wang, 2010). Single-neuron, intracranial, fMRI, and lesion evidence indicates that the DLPFC plays an essential role in WM maintenance (Rottschy et al., 2012; Michels et al., 2010; Altamura et al., 2007; Curtis & D'Esposito, 2003; Manoach et al., 1997). For example, the BOLD fMRI signal in DLPFC is parametrically related to both increases in memory load and task complexity (Rottschy et al., 2012; Michels et al., 2010; Altamura et al., 2007; Jansma, Ramsey, de Zwart, van Gelderen, & Duyn, 2007; Manoach et al., 1997). Similarly, single neurons in DLPFC in macaques exhibit stimulus-selective persistent neural firing across the delay period of WM task (Funahashi, 2017; Riley & Constantinidis, 2016; Lara & Wallis, 2015; Goldman-Rakic, 1995; Fuster, 1973; Fuster & Alexander, 1971). Signatures of such "persistent" activity in DLPFC have also been observed using fMRI in humans (Curtis & D'Esposito, 2003). The importance of human DLPFC in WM is further supported by the effects of stimulating DLPFC with TMS, which can result in profound changes in WM task performance. Depending on the stimulation protocol, such stimulation can result in either enhanced (Bagherzadeh, Khorrami, Zarrindast, Shariat, & Pantazis, 2016) or decreased WM performance (Schicktanz et al., 2015; Morgan, Jackson, van Koningsbruggen, Shapiro, & Linden, 2013). The specific role of the DLPFC in WM is thought to be of an executive—compared with a simple maintenance—nature, that is, it is thought to coordinate and control other WM-related areas, including the hippocampus.

Hippocampal involvement in WM depends on task duration and complexity (Yoon, Okada, Jung, & Kim, 2008) and changes as a function of age (Finn, Sheridan, Kam, Hinshaw, & D'Esposito, 2010). In contrast, pFC appears to be essential for WM task performance at any age and for a wider range of tasks. Moreover, it seems that the DLPFC is primarily engaged in maintaining and processing of information lasting from milliseconds to several seconds, whereas the hippocampus is crucial when WM demands are more complex and/or when maintenance duration is longer (Yoon et al., 2008). In addition, animal studies show that both hippocampal and prefrontal activity during WM tasks is critical (Bähner et al., 2015; Spellman et al., 2015; Yoon et al., 2008). In humans, persistently active cells during WM maintenance have been observed in both the hippocampus and the MFC, but the properties of these cells differ between the two areas. Although persistent activity was observed in both areas, such activity was only stimulus selective in the hippocampus (Kamiński et al., 2017). In contrast, persistent activity in MFC was sensitive to load and memory quality, but not stimulus identity. Together, this existing literature indicates that studying the distinct contributions of different brain areas to WM maintenance is a powerful way to differentiate what a particular area contributes to WM.

Although there is extensive evidence for a role of the DLPFC in WM, it remains unknown whether theta band power in DLPFC is modulated by WM and whether such theta band changes are similar to those observed in the MFC and hippocampus. Here, we utilize intracranial recordings to directly compare the degree of modulation of theta band power in these three areas. We identified contacts placed in the DLPFC in 13 neurosurgical patients and compared the intracranial EEG (iEEG) recorded from these to those obtained from contacts placed in the hippocampus and dACC in the same patients. We found that DLPFC theta band exhibited prominent load-related power decreases, a pattern of change markedly different from that found in hippocampus and dACC. These power decreases were predictive of behavior in a given trial as well as individual differences between participants, indicating that these power reductions were significant for WM maintenance. Together, our results raise the intriguing question of how reductions in power in a given frequency band can be beneficial for the contribution of an area to a particular cognitive function.

## METHODS

### Participants

We recorded iEEG from 13 patients (14 sessions) implanted with depth electrodes for possible surgical treatment of epilepsy. We previously reported single-neuron recordings in the medial temporal lobe and MFC from a subset of the same patients in the same task (Kamiński et al., 2017). Here, in contrast, our focus is on the iEEG signal, in particular on the DLPFC. The average age of our participants was 37.46 years (*SD* = 16.2, 17–70 years); seven patients were men (see Table 1). Patients volunteered for the study and provided informed consent. This study was approved by the institutional review board of the Cedars-Sinai Medical Center.

#### *Localization of Electrodes*

All electrodes were localized based on pre- and postoperative T1 structural MRIs. We used the following processing pipeline to transform the postoperative MRI into the same space as a template brain. We extracted the brains from the pre- and postoperative T1 (Ségonne et al., 2004) scans and aligned the postoperative scan to the preoperative scan with Freesurfer (https://surfer.nmr.mgh.harvard.edu/) *MRI_Robust_Register* algorithm (Reuter, Rosas, & Fischl, 2010). We then computed a forward mapping of the preoperative scan to the CIT168 template brain (Tyszka & Pauli, 2016) using a concatenation of an affine transformation followed by a symmetric image normalization (SyN) diffeomorphic transform, computed by the ANTs software package (Avants et al., 2008). This resulted in a postoperative scan overlaid on a version of the CIT168 template brain (Tyszka & Pauli, 2016) registered in MNI152 space.

We have described our electrode localization procedures for amygdala, hippocampus, and dACC previously (Minxha, Mamelak, & Rutishauser, 2018; Kamiński et al., 2017; Minxha et al., 2017). We have not previously documented our procedures for DLPFC, which are as follows. We compared the locations of putative DLPFC contacts to landmarks that define the boundaries of DLPFC (in Freesurfer Freeview). The boundaries we used followed the standard recommendations for TMS navigation (Mylius et al., 2013): We included electrodes placed in the middle frontal gyrus (MFG) between the superior frontal sulcus and the inferior frontal sulcus (the middle of the line separating the anterior and middle thirds of the MFG; see Mylius et al., 2013). Such location is also in accordance to other definitions based on cytoarchitectonic approach, where DLPFC is defined as BA 46 and BA 9 (Rajkowska & Goldman-Rakic, 1995). Note that, here, we included only contacts in MFG for analysis. However, DLPFC proper also extends into the superior frontal gyrus (BA 9), but no such contacts were included here. It is thus important to note that the results here only pertain the part of DLPFC located in MFG. The location of each contact was confirmed visually, and only contacts located within the defined boundaries were included in the analyses. Applying this approach resulted in 46 contacts identified as DLPFC contacts (two to four per participant, across both hemispheres, zero to two per hemisphere). For dACC and hippocampus, we took the most medial contacts (clinical contact closest to the microwires) on the electrodes targeting the dACC and hippocampus (for each, we confirmed proper microwire placement in the targeted area), respectively. In total, we identified 26 dACC and 23 hippocampus contacts.

For visualization purposes only, electrode locations were projected into MNI152 space and projected onto a 2-D plane by collapsing across the third axis (Figure 1D–E). MNI coordinates for all electrodes are given in Table 2.

**Table 1.** Characteristics of Participants Included in This Study

| *ID* | *Age (years)* | *Sex* | *Epilepsy Diagnosis* |
|---|---|---|---|
| P 34[a] | 70 | M | Bilateral medial temporal |
| P 35[a] | 63 | M | Left temporal neocortical |
| P 36[a] | 45 | M | Right hippocampus |
| P 37[a] | 33 | F | Right hippocampus |
| P 39[a] | 26 | M | Right insula |
| P 40[a] | 25 | M | Right motor cortex |
| P 42 | 25 | F | Not localized |
| P 43 | 42 | F | Left hippocampus |
| P 44 | 53 | F | Right medial temporal |
| P 47 | 32 | M | Right medial temporal |
| P 48 | 32 | F | Left amygdala |
| P 49 | 24 | F | Amygdala |
| P 51 | 17 | M | Not localized |

M = male; F = female.

[a]The behavioral and single-neuron data from these patients are also part of Kamiński et al. (2017), but the depth electrode recordings analyzed here are unpublished in all patients included.

### Stimuli and Procedures

#### *Task*

Participants performed a WM task ("Sternberg" task, based on Sternberg, 1966). In each trial, participants were asked to remember between one up to three sequentially presented pictures. Then, after 2.5–2.8 sec of maintenance period, they were presented with another picture and asked if they have seen it or not. We used a modified Sternberg task with images (instead of the usual digits) as material for memorization (Figure 1A). Each trial started with a fixation cross shown for 900–1000 msec. Next, we sequentially presented the images to be memorized ("encoding") in a given trial. Each picture was presented for

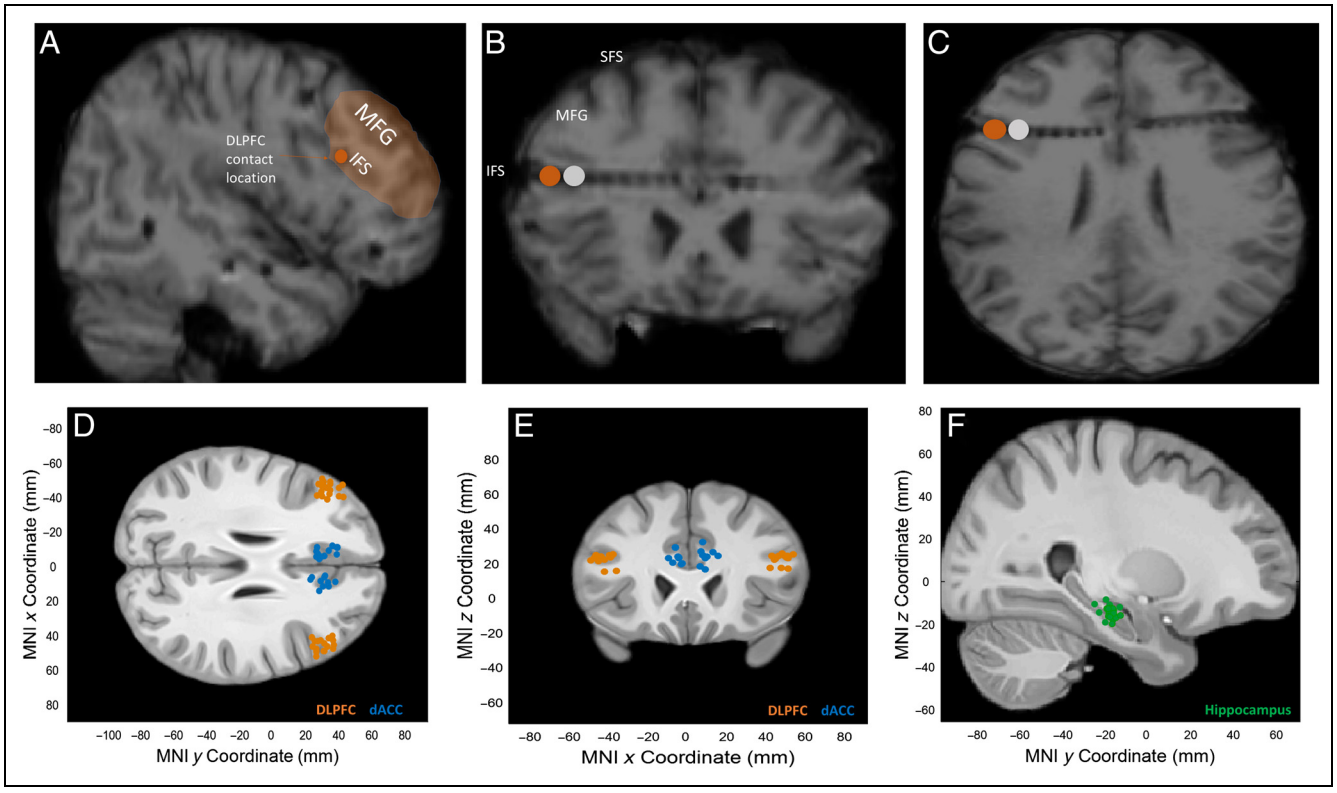


**Figure 1.** Electrode localization. (A–C) Illustration of DLPFC electrode in one individual brain (P37CS). MFG = medial frontal gyrus; IFS = inferior frontal sulcus; SFS = superior frontal sulcus. Orange shows the active contact; gray shows the reference contact used for analysis. (D–F) Summary of all recording locations, shown in MNI152 space displayed superimposed on the California Institute of Technology's CIT168 T1w brain atlas (Tyszka & Pauli, 2016). Recording locations are indicated by different colors (D, E: orange, DLPFC; blue, dACC; F: green, hippocampus).

1 sec, followed by a blank screen for 1–200 msec (randomized). Participants were asked to memorize the one to three images shown in each trial. After encoding, there was a maintenance (delay) period lasting at least 2.5 sec and at most 2.8 sec. During this time, the word "hold" was shown on the screen. Lastly, after the end of the maintenance period, a probe stimulus was displayed, and participants were asked to decide whether the probe stimulus has been presented in the encoding phase. Participants responded by pressing the green or red buttons on a response pad. Which color corresponded to "yes" and which color corresponded to "no" were shown at the top of the screen during each probe trial (Figure 2). We used this approach to switch the location of the yes and no buttons in the middle of the experiment as a control. We asked participants to respond as fast as possible. The probe picture was presented until participants made a response. In each session, participants performed 108 (first participant) or 135 (all participants except the first one) trials, depending on the task variant (we changed the number of trials from 108 to 135 after the first participant). Pictures were shown in pseudorandom order. A schematic overview of the task is shown in Figure 2. The number of pictures presented in a given trial was unknown to the participant (the load variable was mixed within blocks).

### *iEEG Measurement and Analysis*

We recorded broadband (0.1–500 Hz filter) and continuous signals from all channels sampled at 2 kHz using a Neuralynx Atlas system. Recordings were referenced to a subgaleal reference electrode strip (Minxha et al., 2018). Data analysis was performed offline using EEGLAB toolbox (Delorme & Makeig, 2004) and custom MATLAB (The MathWorks, 2015) scripts. The continuous iEEG was downsampled to 500 Hz, and the recording channels of interest were re-referenced to bipolar by subtracting the signal of the contact closest to the channel of interest (see Figure 1). For DLPFC electrodes, this was the immediate next medial channel to the channel of interest (see Figure 1B and C), whereas for hippocampus and dACC, this was the immediate next lateral channel on the same electrode. Next, we $z$-transformed the signal of each channel separately. The 4500-msec-long epochs were then extracted from the maintenance period of every trial (starting 1000 msec before the start of maintenance till 1000 msec after the end of the maintenance period, which lasted at least 2500 msec), and 3000-msec epochs were extracted from the picture presentation period (encoding) as well as from the retrieval period (starting 1000 msec before and ending 1000 msec after the actual 1000-msec lasting periods of interest). For the

**Table 2.** Coordinates for Each Electrode Used in Analyses

| *ID* | *Right DLPFC* | *Left DLPFC* | *Right Hippocampus* | *Left Hippocampus* | *Right dACC* | *Left dACC* |
|---|---|---|---|---|---|---|
| P 34 | 43.78, 23.23, 23.43; 49.08, 23.85, 23.43 | −40.73, 24.47, 24.95; −47.43, 25.45, 25.10 | 30.56, −16.81, −16.47 | −29.78, −17.97, −13.35 | 6.81, 21.20, 32.38 | −7.20, 24.71, 29.13 |
| P 35 | 40.72, 33.64, 30.99; 45.76, 34.48, 30.48 | N/A | 29.80, −14.88, −12.13 | N/A | 5.78, 29.40, 27.02 | −6.83, 36.47, 27.02 |
| P 36 | 43.24, 34.34, 21.69; 48.29, 34.24, 21.36 | −39.89, 40.26, 24.02; −46.94, 40.07, 23.38 | N/A | −31.43, −20.12, −14.96 | 9.15, 35.35, 22.12 | −10.70, 36.91, 23.29 |
| P 37 | 41.65, 21.43, 24.43; 46.89, 21.68, 25.31 | −40.04, 27.72, 23.63; −45.28, 29.33, 23.63 | 28.83, −20.52, −13.51 | −30.27, −19.20, −12.19 | 7.96, 20.70, 23.04 | −10.78, 24.45, 23.37 |
| P 39 | 43.26, 26.67, 22.42; 49.53, 28.48, 24.65 | −37.24, 25.88, 15.70; −43.26, 25.88, 15.56 | 32.51, −26.99, −10.51 | −28.92, −18.21, −12.85 | 14.70, 25.70, 24.68 | −5.25, 27.04, 23.46 |
| P 40 | 48.15, 24.17, 24.49; 52.79, 24.08, 25.23 | −46.00, 27.42, 21.47; −50.23, 27.42, 21.82 | 33.93, −19.63, −10.91 | −30.49, −20.39, −16.20 | 12.07, 28.21, 26.50 | −8.53, 23.81, 20.78 |
| P 42 | 45.07, 28.97, 24.49; 49.52, 28.97, 24.49 | −41.64, 32.06, 22.09; −47.47, 32.40, 22.09 | 30.59, −21.51, −8.30 | −24.64, −21.10, −12.78 | 6.81, 28.80, 24.92 | −3.95, 28.42, 19.54 |
| P 43 | 43.70, 24.70, 22.77; 49.86, 24.02, 23.12 | −43.01, 27.10, 22.43; −48.49, 28.29, 23.12 | 31.40, −24.80, −14.60 | −30.15, −20.34, −12.68 | 8.76, 26.85, 23.89 | −5.25, 23.95, 23.39 |
| P 44 | 43.40, 31.42, 16.99; 49.93, 29.92, 16.99 | −43.10, 37.38, 15.36; −48.48, 36.63, 14.46 | 29.40, −21.70, −19.07 | −25.29, −16.88, −17.11 | 5.20, 30.60, 18.63 | −10.68, 36.48, 20.17 |
| P 47 | 40.95, 30.18, 17.46; 46.49, 30.18, 17.77 | N/A | 30.37, −18.10, −18.10 | −30.86, −17.82, −14.70 | 8.12, 26.02, 16.64 | −3.89, 25.92, 20.00 |
| P 48 | 44.31, 37.38, 18.41; 50.25, 37.07, 18.28 | −38.58, 30.60, 25.32; −44.93, 30.12, 23.90 | N/A | −34.46, −14.83, −15.94 | 11.72, 38.61, 17.97 | −5.88, 28.68, 24.07 |
| P 49 | N/A | −40.01, 37.91, 21.56; −45.03, 37.91, 20.54 | 29.25, −17.87, −14.78 | −24.15, −18.71, −19.93 | 9.56, 31.04, 26.12 | −11.37, 33.91, 25.24 |
| P 51 | 41.79, 31.65, 26.49; 46.88, 30.53, 25.62 | −43.58, 32.35, 26.67; −48.68, 32.35, 26.26 | 29.86, −17.98, −13.83 | −30.47, −19.73, −16.72 | 11.90, 31.65, 25.50 | −8.78, 31.45, 28.02 |
| Avg | *x*: 46.05 (3.4) | *x*: −44.09 (3.67) | *x*: 30.59 (1.52) | *x*: −29.24 (3.06) | *x*: 9.12 (2.8) | *x*: −7.62 (2.7) |
| | *y*: 28.97 (4.79) | *y*: 31.32 (5.02) | *y*: −20.07 (3.55) | *y*: −18.78 (1.77) | *y*: 28.8 (5.06) | *y*: 29.4 (5.06) |
| | *z*: 22.95 (3.84) | *z*: 21.93 (3.59) | *z*: −13.83 (3.28) | *z*: −14.95 (2.33) | *z*: 23.8 (4.25) | *z*: −23.65 (3.08) |

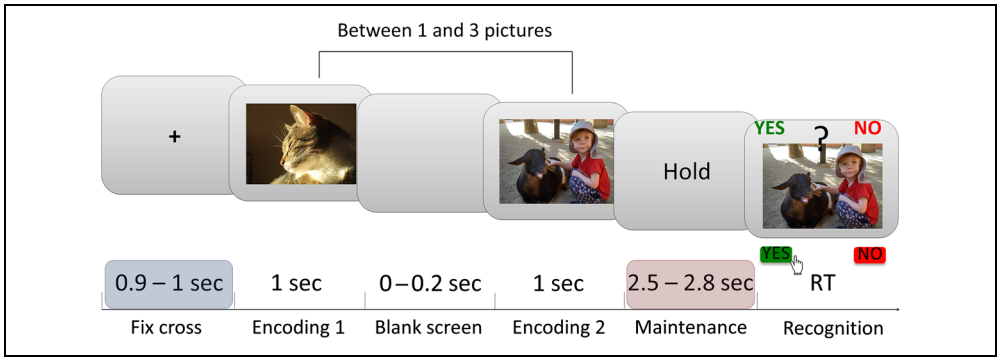


**Figure 2.** The task. Top: example of the screens presented to the participants during an example trial (here with Memory Load 2). Bottom: the duration for which each screen was shown. Each trial started with an encoding phase, during which between one and three sequentially presented pictures were shown. This was followed by the maintenance (delay) period. Finally, after the delay, a probe image was shown. Participants were asked to indicate whether the probe was or was not shown during the encoding period that immediately preceded the probe. All analysis shown in this article was performed during the maintenance and baseline periods (red and blue, respectively).

baseline, we extracted a 2000-msec-long segment for every trial (1000 msec before up to 500 msec after the actual baseline period, which was defined as a 500-msec period of time with fixation cross before the first picture presentation; see Figure 2 where it is marked with a blue shading on the experiment's time line). All trials were visually inspected for artifacts and rejected if found to contain artifacts (with an average of 87 ± 0.8% of epochs remaining in the analysis). We used the Morlet continuous wavelet transform (CWT; 16 scales per octave, minimum period to analyze was set to 0.01 and maximum period was set to 0.8) as implemented in WAVOS (Wavos 2.3.1) to calculate the absolute power spectral density for every trial. We first computed the CWT on the entire trial and then extracted the periods of interest as described above. Finally, we transformed the units of power to decibels relative to the average power during the baseline period.

### *Statistical Analyses*

For comparisons between two conditions, we used the permuted *t*-test statistic. For comparisons with more than two conditions, we used permuted *F* statistic. Note that we used permutation tests throughout to avoid the assumption of normality. As a result, note that the reported *p* values may differ from those expected from the parametric *t* and *F* distributions because *p* values were based on the empirically estimated null distribution. We used corrections for multiple comparisons based on cluster-based approach (Maris & Oostenveld, 2007), when appropriate. For linear mixed-effects models and correlation analysis, we used MATLAB's *FITLME* function and Spearman's rho, respectively.

## RESULTS

### Behavioral Data

Participants ($n$ = 13 in 14 sessions) performed the task well: Overall accuracy was 87.57 ± 4.33%, with a median RT (for correct trials only) of 1.07 ± 0.27 sec. As expected (Sternberg, 1966), accuracy decreased (Figure 3A; $F(2, 26) = 3.65$, $p = .037$, permuted repeated-measures ANOVA) and RT increased (Figure 1B; $F(2, 26) = 6.69$, $p = .0025$, permuted repeated-measures ANOVA) as a function of the number of items held in memory (here referred to as load). Also, RT was significantly faster for correct compared with incorrect trials (Figure 3C; permuted paired $t$ test: $t(13) = 6.26$, $p = .005$, using trials from Load 3 only due to low error rates for low loads; average error rates were 0.066, 0.093, and 0.12 for Loads 1, 2, and 3, respectively). Together, this pattern of behavioral results shows that our patients performed the task accurately and exhibited the expected patterns of accuracy and RT differences (Sternberg, 1966). For all subsequent analysis, we used only correct trials unless indicated otherwise. We did observe minor but nonsignificant priority and recency effects (in Load 3 trials, the image presented last was recognized faster [$M$ = 1.16 sec] than the image presented in the middle [$M$ = 1.32 sec]). Similarly, the image presented first during encoding was recognized faster ($M$ = 1.23 sec) relative to the middle image. However, these differences were not statistically significant, $F(2, 26) = 1.47$, $p = .25$.

### Electrophysiology

Across 13 patients, we recorded from a total of 46, 26, and 23 channels in DLPFC, dACC, and hippocampus, respectively (see Methods section and Table 1). We localized electrode contacts based on postoperative MRI scans and only included channels confirmed to be in either area (see Methods section and Figure 1 for definition of what we included as DLPFC). All analyses conducted in this article was performed on bipolar-referenced recordings (referenced to the immediate next contact relative to the one of interest, see Methods section).

### Changes in Power Spectrum during Maintenance versus Baseline

As a first step, we compared whether the patterns of power changes during the maintenance period relative to the

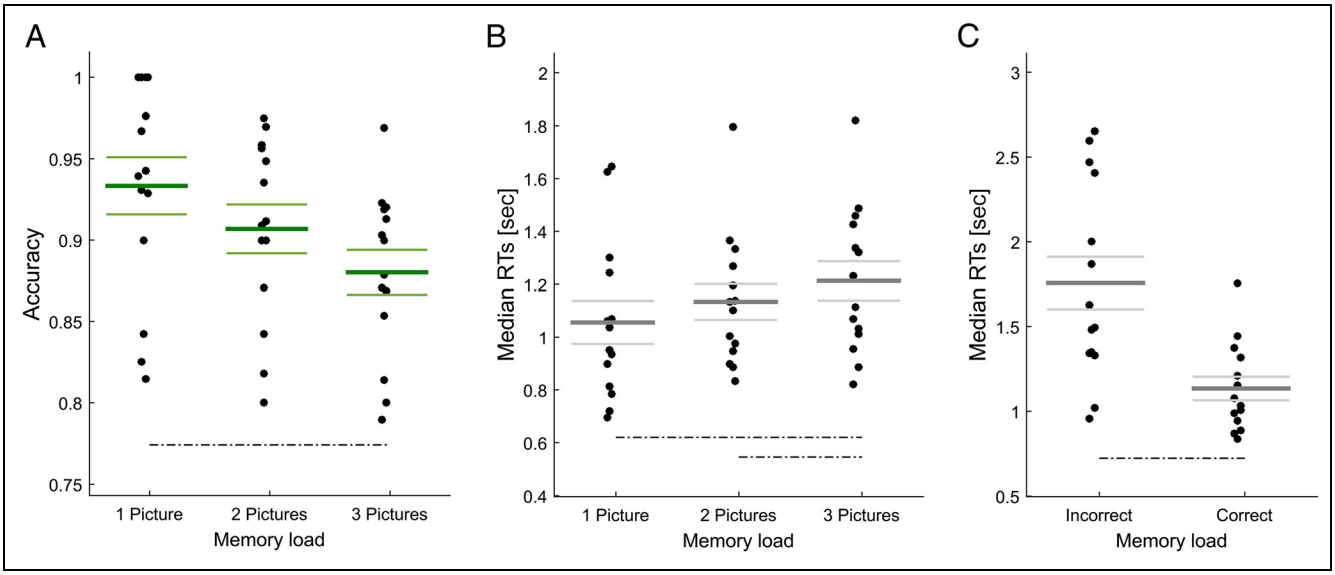


**Figure 3.** Behavioral results. (A) Accuracy decreased as a function of load. (B) RT increased as a function of load. (C) RT differed significantly between correct and incorrect trials. C only includes data from Load 3. Each dot shows one session. Dotted lines indicated significant pairwise differences at $p < .05$.

baseline period differed between brain areas. We performed a permuted 1 × 3 ANOVA for power at each frequency, corrected for multiple comparisons using a cluster-based approach (Maris & Oostenveld, 2007). Results at $p < .05$ were considered statistically significant. Averaging across all loads, we found that the pattern of response in the broadband power varied systematically between the three brain areas investigated here. Whereas in DLPFC we found broadband decreases relative to baseline, in both dACC and hippocampus we observed significant power increases relative to baseline (Figure 4A). In a pairwise comparison between the brain areas, this difference was significant between DLPFC and hippocampus in the 1–20 Hz band (Figure 4B). Comparing between DLPFC and dACC, power was significantly different in the 1–15 Hz band (Figure 4C). In contrast, differences between dACC and hippocampus were only significant in the 12–20 Hz band, with no significant differences in the 1–5 Hz band (Figure 4D). Together, this shows significant and relatively broad band power deceases in DLPFC and power increases in the dACC and hippocampus during WM maintenance relative to baseline. As a further control, we also assessed whether the raw power (rather than subtracted from baseline or between loads, as reported above) in DLPFC differed relative to that expected from the background 1/*f* spectrum. This revealed that raw power differed significantly from the background in both the theta and beta frequency band (Figure 4E) and that the power decreases relative to baseline were also apparent in the raw spectra.

### Changes in Theta Power as a Function of Load

We next investigated whether maintenance-related activity varied as a function of load—a strategy commonly used in investigating the mechanisms of WM (Hsieh & Ranganath, 2014; Roux & Uhlhaas, 2014; Meltzer et al., 2008; Onton et al., 2005). So, in the next analysis, we asked whether the power increases/decreases we described above scaled as a function of load by comparing the magnitude of change between high (three items) and low (one item) load conditions (Figure 5). This revealed that the extent of DLPFC power decreases was a function of load, with the largest decrease for the high load condition (permuted ANOVA, $p = 7.1418e{-}05$, 3.29–6.86 Hz, corrected for multiple comparisons). In contrast, the higher the load, the larger the increase in theta band power in the hippocampus (permuted ANOVA, $p = .038$, 2.43–3.91 Hz, without correction for multiple comparisons, after correction all effects were statistically nonsignificant). It was notable that the effect size was substantially larger in the DLPFC relative to the hippocampus ($d_{\text{DLPFC}} = 0.961$, $d_{\text{HIPPOCAMPUS}} = 0.477$). An additional difference was that the load modulation in DLPFC was most apparent in a higher frequency compared with the hippocampus (5 Hz vs. 3.5 Hz). Lastly, the pattern of response in the dACC did not vary significantly as a function of memory load (but note that, relative to baseline, power increased significantly in the dACC, but this change was not a function of load). Together, this shows that the power increases and decreases in hippocampus and DLPFC during maintenance were modulated significantly by memory load, but this modulation was of opposite sign for DLPFC (negative) compared with hippocampus (positive). This analysis also shows that, in contrast to the comparison maintenance period versus baseline, the load-related scaling was specific to the theta frequency band (the first, more general comparison revealed a broadband effect).

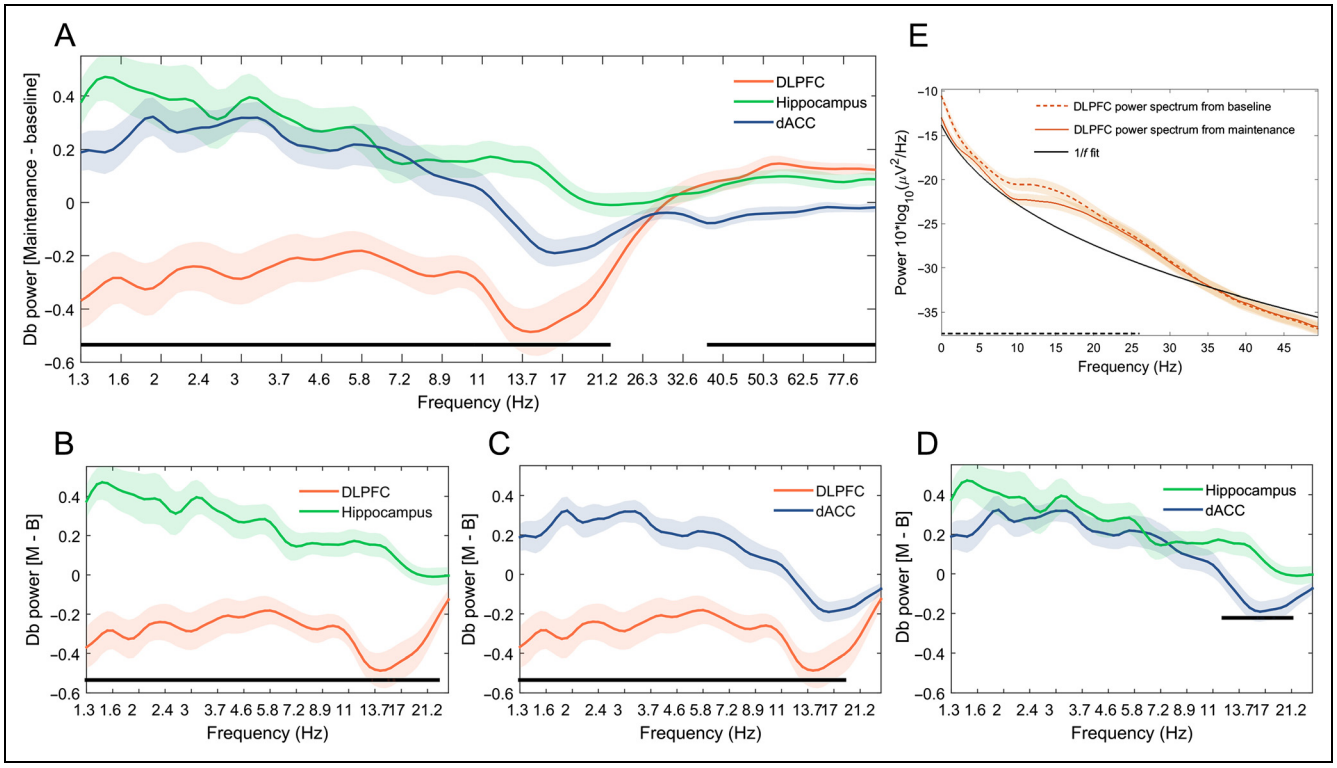


**Figure 4.** Broad band power changes relative to baseline during maintenance. Spectral comparisons between task (maintenance period) and baseline for DLPFC, hippocampus, and dACC showing contrasting effects between neocortex (DLPFC) and allocortex (hippocampus and dACC). Plots show averaged power during maintenance in units of decibels (dB) relative to baseline across all electrodes in a given brain area. (A) Power as a function of frequency for DLPFC, dACC, and hippocampus. Significance indicated is the result of a 1 × 3 ANOVA at $p < .05$. (B–D) Pairwise differences between brain areas. Significance indicated is computed using post hoc tests (permuted $t$ tests). All significant data points marked as a black line are significant at $p < .05$ and corrected for multiple comparisons using a cluster-based approach (Maris & Oostenveld, 2007). In DLPFC, the difference was negative (decrease in power during maintenance relative to the baseline) and most pronounced at 2 Hz ($p = .0012$), 3 Hz ($p = .0062$), and then 6.5 up to 20 Hz ($p = .0012$). In hippocampus, the difference was positive (increase in power during maintenance compared with the baseline period) and most pronounced between 2.8 and 6.3 Hz ($p = .0012$). In dACC, the difference was positive in lower bands (increase in power during maintenance compared with the baseline period, between 2 and 6.5 Hz, $p = .0012$) and negative in higher bands (decrease in power during maintenance relative to the baseline, between 15 and 22 Hz, $p = .0012$). (E) Raw power spectra from maintenance and baseline periods of the task for DLPFC. The black dotted line denotes statistically significance of the difference between the expected 1/*f* background and the measured DLPFC power spectra (1 × 3 permuted repeated-measures ANOVA corrected for multiple comparisons using cluster-based approach).

We next asked whether the extent of theta power increase/decrease was indicative of memory load for individual electrodes (rather than averaged across as shown above). For this analysis, we averaged power in the frequency of interest (3–6 Hz theta band) for each electrode and for each memory load separately. We then performed a 3 (Memory load: 1 picture vs. 2 pictures vs. 3 pictures) × 3 (Area of interest: DLPFC vs. dACC vs. hippocampus) repeated-measures ANOVA with Theta power as the dependent variable. We found that the main effects of Memory load, $F(2, 200) = 4.46$, $p = .013$, $\eta^2 = .043$, and Brain area, $F(2, 100) = 15.086$, $p < .0001$, $\eta^2 = .232$, as well as the interaction, $F(4, 200) = 10.73$, $p < .0001$, $\eta^2 = .177$, were statistically significant, demonstrating the robustness of this effect at the single-electrode level. The significant interaction effect was due to the opposite pattern of effects for DLPFC (see Figure 6A; where we observed a significant, negative linear trend: $F(1, 49) = 49.24$, $p < .0001$, $\eta^2 = .501$) compared with hippocampus (see Figure 6B; where the trend was significant but much weaker and positive: $F(1, 24) = 5.18$, $p = .032$, $\eta^2 = .178$) and dACC (see Figure 6C; $F < 1$, *ns*). See also Figure 8 for additional single-channel presentation of this effect.

We next confirmed this conclusion at the single-trial level. For this, we used a linear mixed-effects model with memory load and brain area as fixed factors and channels as random factors. Theta power in each trial constituted the dependent variable. The goal of this analysis was to confirm the Brain Area × Memory Load interaction on the single-trial level. We found that the interaction term was highly significant, $F(1, 11950) = 45.55$, $p = 1.5584e{-}11$. This confirms the robustness of the opposite effects of load on theta power in the DLPFC versus dACC/hippocampus at the single-trial level.

We performed several control analyses to exclude potential confounds. First, we verified whether evoked responses (ERPs) to the onset of the waiting period ("hold" instruction) differed between loads. To do so, we averaged the raw signal across trials from each load

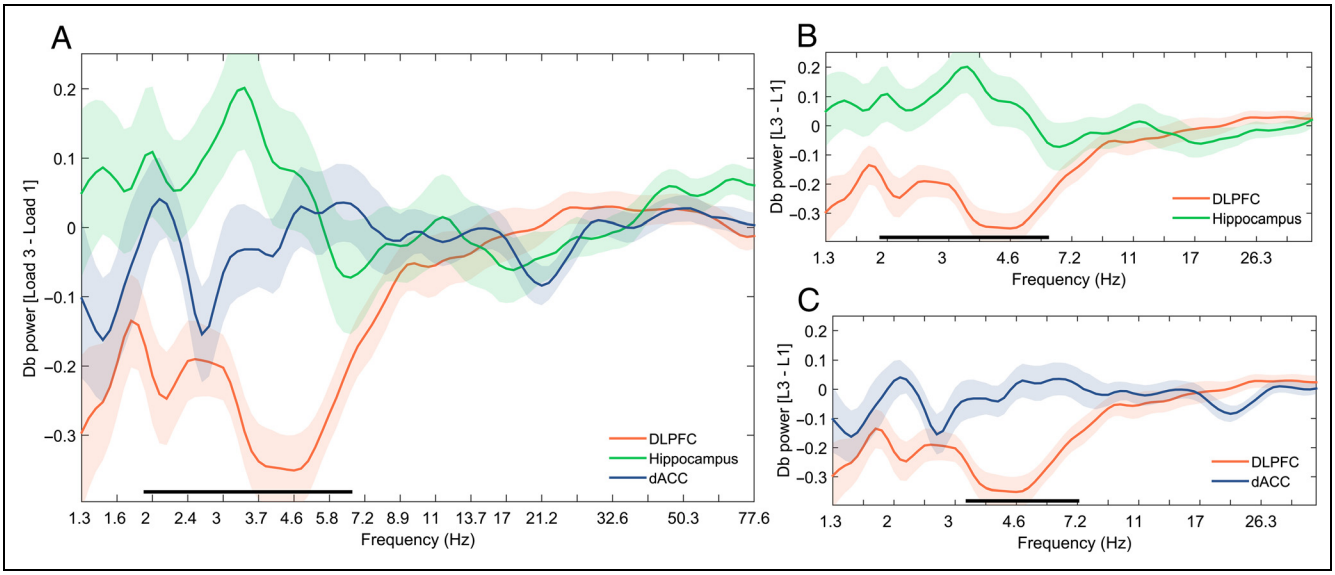


**Figure 5.** Theta band power is modulated by load during maintenance. (A) Differences in power between Loads 3 and 1, averaged across all electrodes located in a given brain area (correct trials only). Each line represents the difference in power between trials with high (three pictures in memory) and low memory load (one picture in memory). Black line indicates significant differences between the three areas as indicated by a 1 × 3 ANOVA at $p < .05$. (B, C) Pairwise comparisons between DLPFC and hippocampus (B) and DLPFC and dACC (C). Black line indicates significant differences derived from post hoc tests at $p < .05$ (permuted $t$ tests for independent samples). The comparison between hippocampus and dACC did not reveal statistically significant differences and is not shown. All comparisons were performed with correction for multiple comparisons using cluster-based approach (Maris & Oostenveld, 2007).

separately and then submitted these ERPs to a permuted repeated-measures ANOVA (we compared ERPs independently at every point of time, corrected for multiple comparisons using a cluster-based approach; Maris & Oostenveld, 2007). This analysis revealed that ERPs from different loads did not differ statistically significantly at any point of time. Second, we confirmed that those evoked responses did not cause the reported load-related theta power changes in DLPFC. To achieve this, we subtracted the ERPs from each individual trial of a given load and repeated the above analysis on the resulting ERP-subtracted trials. Compatible with the original analysis, this again revealed a significant effect of Memory load on DLPFC theta power: $F(2, 98) = 31.28$, $p < .0001$

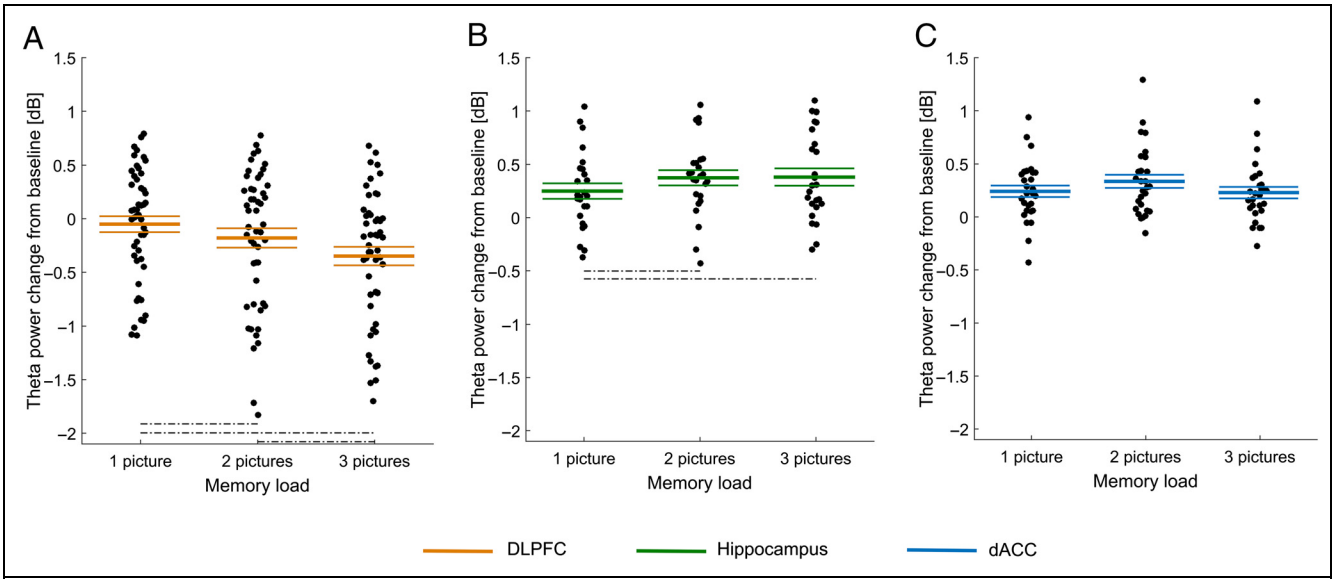


**Figure 6.** Theta (3–6 Hz) power modulation by memory load in DLPFC, hippocampus, and dACC. Changes of theta power as a function of load quantified at the single-electrode level (each dot is an electrode). (A) DLPFC theta power decreases significantly as a function of load (see text for statistics). (B) In hippocampus, theta power increased significantly as a function of load, but the strength of this modulation was significantly weaker compared with that in DLPFC (see A). (C) In dACC, we found no significant effect of memory load on theta power (but note that, for each load, power is significantly stronger then baseline). Dashed lines denote statistically significant differences at $p < .05$.

($M_{load1} = -0.54$; $M_{load2} = -0.68$; $M_{load3} = -0.84$). In comparison, the effect sizes of the original analysis (where the ERP was not subtracted) were similar, $F(2, 98) = 30.41$, $p < .0001$ ($M_{load1} = -0.93$; $M_{load2} = -1.06$; $M_{load3} = -1.23$). Together, this shows that the load-dependent theta power decrease in the DLPFC was not related to an evoked response.

### Time Course of DLPFC Power Changes

We next investigated how theta power in the DLPFC is changing over the course of the task. We were especially interested in whether changes in theta power were also visible during the encoding or retrieval stage and how power changes evolved throughout the maintenance period. We found that, throughout the maintenance period, theta band power scaled as a function of load, with less power for higher loads (Figure 7A, middle). Also, during encoding, theta band power dropped in a stepwise fashion as more items were encoded (Figure 7A, left). Notable, neither the beta (see Figure 7B) nor the gamma (see Figure 7C) frequency band showed similar load-related changes during maintenance.

### Theta Power as a Predictor of Task Performance

In the analysis above, we considered only correct trials. We next asked whether there is a relationship between theta power and performance (we tested accuracy and RT). To test for effects of accuracy, we used a linear mixed-effects model. We used Brain area and Accuracy (correct/incorrect) as fixed factors, Channel number as a random factor, and single-trial theta power as the dependent variable. We only used Load 3 trials for this analysis (to have enough error trials). This model revealed significant main effects of both Brain area, $F(1, 4106) = 9.56$, $p = .0019$ (as expected from above analysis), and Accuracy, $F(1, 4106) = 7.61$, $p = .0058$, and a significant interaction between the two, $F(1, 4106) = 3.87$, $p = .049$. Post hoc analysis revealed a significant difference between correct and incorrect trials only in DLPFC, in which correct trials were characterized by lower theta power compared with incorrect trials, $F(1, 1982) = 12.87$, $p = .00034$. We found no significant difference between correct and incorrect trials for theta power in hippocampus and dACC: $F(1, 1004) < 1$, *ns* and $F(1, 1118) < 1$, *ns*, respectively (see Figure 9A–C). Together, this shows that the extent of theta power decreases in DLPFC is predic-

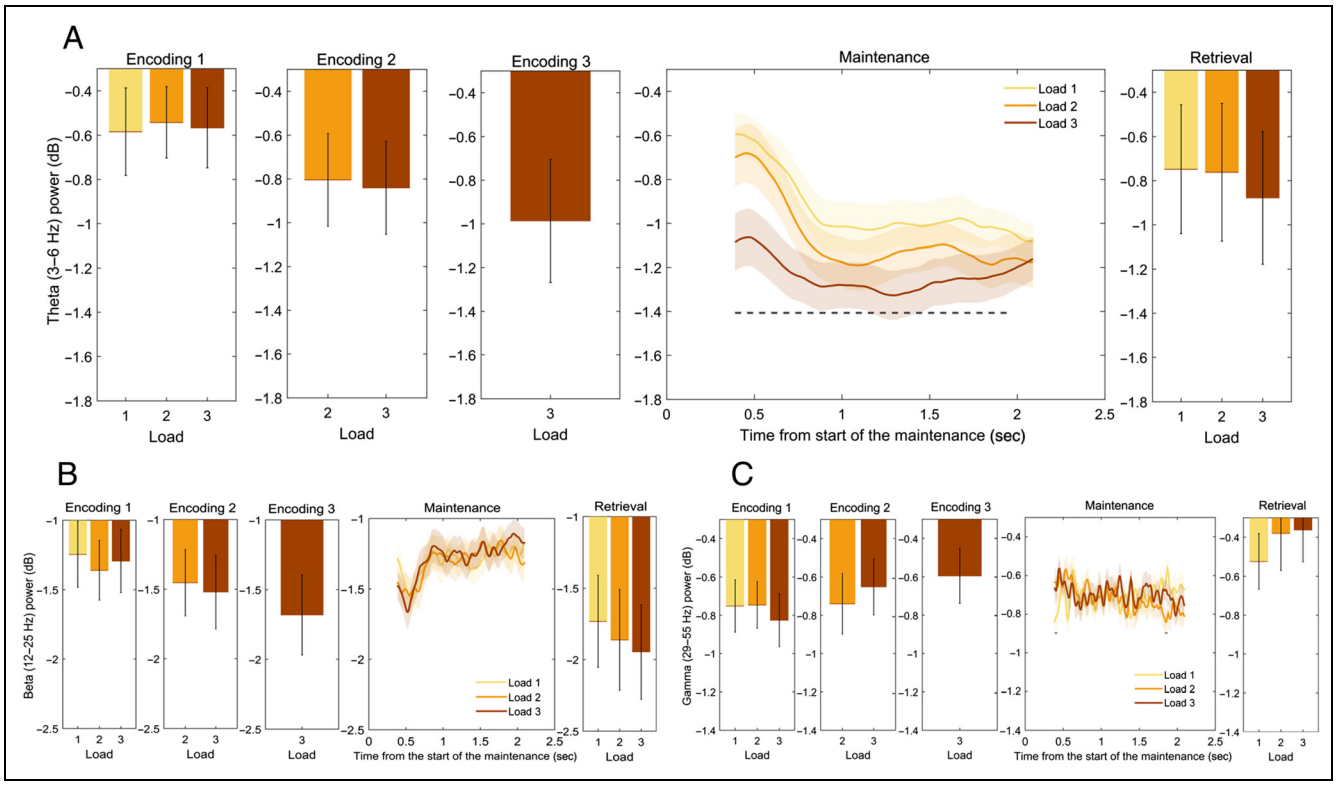


**Figure 7.** Theta, beta, and gamma power time courses throughout the task in DLPFC. Power changes as a function of time for (A) theta, (B) beta, and (C) gamma band. Power was calculated with the Morlet CWT (16 scales per octave, minimum period to analyze was set to 0.01 and maximum period was set to 0.8) as implemented in WAVOS (Wavos 2.3.1) and then transformed to decibels relative to the average power during the baseline period. To avoid contamination from visual transients, we only used the time period starting at 400–2100 msec following the start of the maintenance period to compute power. For the same reason, to calculate the power in the encoding and retrieval periods (bars), we used a time window of 200–1000 msec following image onset. Note that significant load differences during maintenance are only apparent in the theta band (A). All $p$ values are based on permuted repeated-measures ANOVA corrected for multiple comparisons using a cluster-based approach (dashed line denotes at which time points differences are statistically significant).

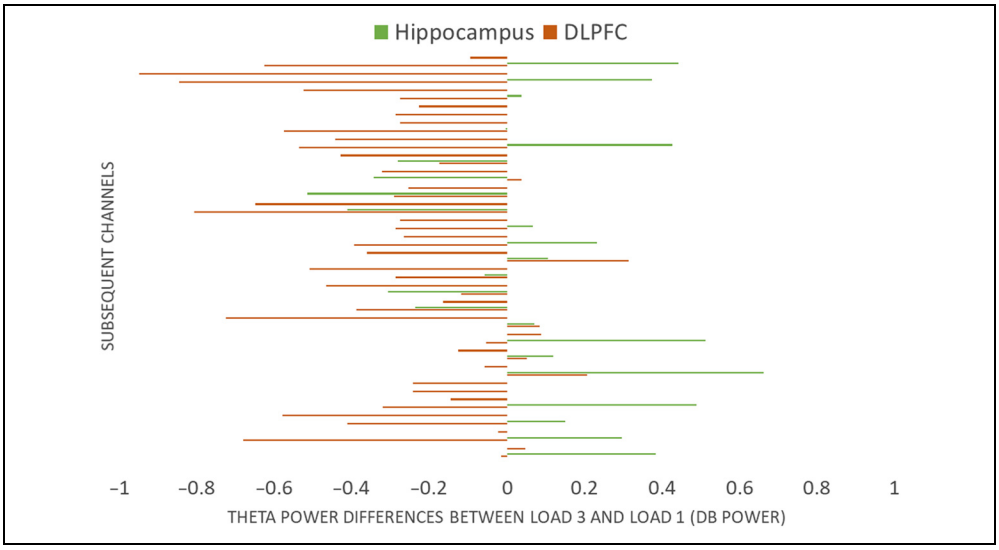


**Figure 8.** Theta power modulation by memory load on individual electrodes from DLPFC and hippocampus. Illustration of the modulation of theta power as a function of load individually for all recorded electrodes recorded in DLPFC and hippocampus, ordered as recorded (from top to bottom, oldest at top). Of the 23 hippocampal channels, 12 showed increases. Of the 48 DLPFC channels, 34 showed decreases.

tive of accuracy, with less power indicative of a higher likelihood of a correct response.

To test for effects of RT, we performed a similar analysis but using only correct trials from all loads. We first ran a linear mixed-effects model with Raw RTs (removing outliers; see Methods section) and Brain area as fixed factors, channels as random factor, and Theta power as the dependent variable. This analysis revealed significant

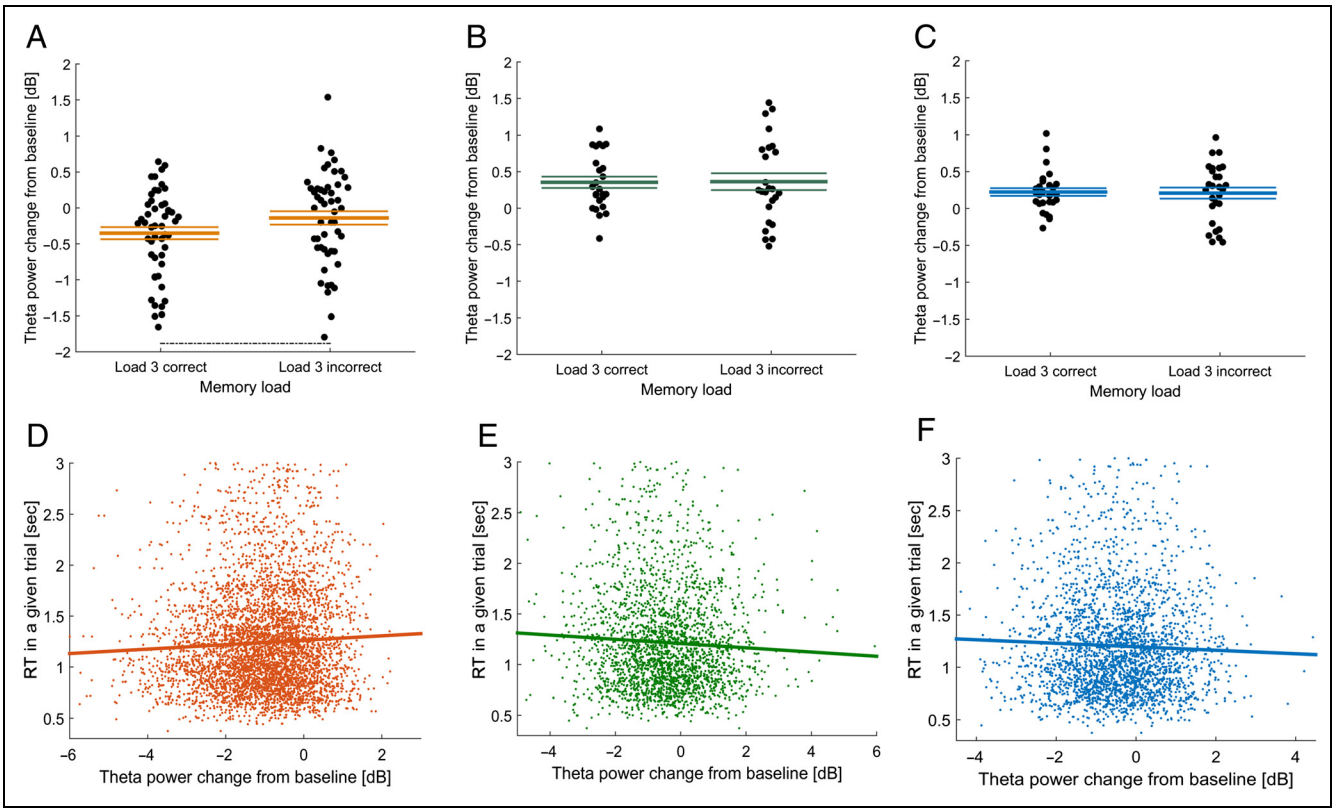


**Figure 9.** Theta power as a predictor of task performance. (A–C) Comparison of theta power change from baseline in correct versus incorrect trials (in Memory Load 3 trials only) for (A) DLPFC, (B) hippocampus, and (C) dACC (each dot is an electrode; dashed lines denote statistically significant differences at $p < .05$). (D–F) The relationship between RT and theta power change from baseline for all trials in (D) DLPFC, (E) hippocampus, and (F) dACC (each dot is a trial). All relationships were statistically significant, post hoc to the main analysis (linear mixed-effects model with RT and Brain area as fixed factors, Channels as random factor, and Theta power as the dependent variable): DLPFC, $r = .052$, $p = 3.2949e-04$; hippocampus, $r = -.056$, $p = .0053$; AC, $r = -.04$, $p = .0358$. To exclude potential confounds of load on RT (the larger the load, the longer the RT), we repeated a linear mixed-effects model analysis after first classifying RTs as below/above the median RT for each load of a given patient—this analysis yielded nearly identical results to the original one.

main effects of Brain area, $F(1, 9980) = 70.51$, $p = 5.2158e-17$, RTs, $F(1, 9980) = 5.96$, $p = .015$, as well as a significant interaction, $F(1, 9980) = 13.86$, $p = .00019$. Post hoc analysis revealed that the interaction effect was due to the opposite sign of the relationship between theta power and RTs in DLPFC (Figure 9D; $r = .052$, $p = 3.2949e-04$) as compared with hippocampus (Figure 9E; $r = -.056$, $p = .0053$) and dACC (Figure 9F; $r = -0.04$, $p = .0358$).

To exclude potential confounds of load on RT (the larger the load, the longer the RT), we repeated above analysis after first classifying RTs as below/above the median RT for each load of a given patient. Thus, for each load, a trial was labeled as either "faster" or "slower" relative to the median RT of that load (a technique we used before; Kamiński et al., 2017). This analysis yielded very similar results: There were significant main effects of Brain area, $F(1, 9980) = 67.19$, $p = 2.7753e-16$, RT, $F(1, 9980) = 12.17$, $p = .00049$, and a significant interaction, $F(1, 9980) = 14.39$, $p = .00015$, resolving the question about the memory load as a potential confound variable. Post hoc analysis again confirmed the opposite signs of modulation due to RT of DLPFC relative to hippocampus and dACC (positive in DLPFC, $r = .052$, $p = 3.2949e-04$; negative in hippocampus, $r = -.056$, $p = .0053$; negative in dACC, $r = -.04$, $p = .0358$). Together, this analysis shows a robust relationship between decreases in theta power in the DLPFC with both accuracy and RT. The directionality of this effect in the DLPFC was such that the more theta power was reduced, the faster and more accurate was the response. In contrast, faster RTs in the hippocampus and dACC were correlated with increases in theta power, and such increases did not correlate significantly with increases in accuracy.

A

| | DLPFC (N = 50) | Hippocampus (N = 25) | dACC (N = 28) |
|---|---|---|---|
| *RTs* | | | |
| *Overall (all loads)* | 0.432** | 0.009 | −0.118 |
| *Load 1* | 0.393** | 0.01 | −0.137 |
| *Load 2* | 0.399** | −0.123 | 0.004 |
| *Load 3* | 0.454*** | 0.089 | −0.171 |
| *Accuracy* | 0.088 | −0.115 | −0.064 |

B

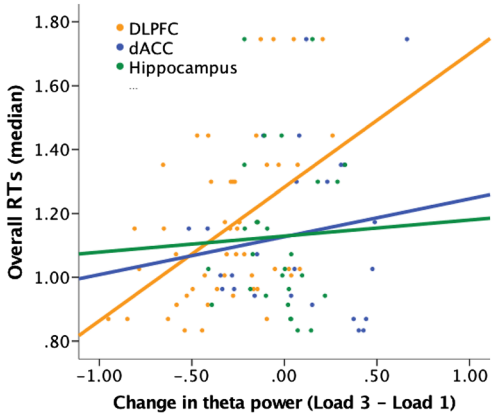


**Figure 10.** Change in theta power in DLPFC as a predictor of individual differences in WM performance. (A) Correlation coefficients between the amount of theta power change and task performance (RT and accuracy). (B) Correlations between theta power change with memory load and individual patient's reaction times for each area. Each dot is an electrode.

### Individual Differences in Load-related Theta Power Changes as a Predictor of Task Performance

We next tested whether the amount of load-related changes in theta power is related to individual differences in RT and accuracy between participants. Note that, in contrast to the within-subject analysis presented so far, what follows is a between-subject analysis. As the neural metric of interest, we again used the difference between theta power in Load 3 relative to Load 1 (for each channel). To quantify behavior, we used accuracy and RT for each participant. We used a linear mixed-effects model with the change in theta power and brain area as predictors and RTs or accuracy as the dependent variable.

For RT, we found a significant main effect of Theta power change, $F(1, 99) = 6.22$, $p = .014$, and Brain area, $F(1, 99) = 4.84$, $p = .036$, with no significant interaction between the two, $F(1, 99) = 2.53$, $p = .115$. When we repeat this analysis with RT from the Load 3 only (the most difficult condition), both main effects were of similar magnitude, $F(1, 99) = 6.98$, $p = .009$, for Theta change and Brain area, $F(1, 99) = 4.8$, $p = .031$, but interaction effect became marginally significant, $F(1, 99) = 3.56$, $p = .062$. To explore this relationship in more depth, we conducted post hoc analyses with only one predictor (theta change) for each area separately. This analysis revealed that the extent of Theta power change was predictive of RTs, but only for DLPFC: $F(1, 48) = 13.19$, $p = .00068$ for RTs from all correct trials and $F(1, 48) = 12, 82$, $p = .00079$ for RT from Load 3. In contrast, for hippocampus and dACC, this effect was not significant (see Figure 10B, C): $F(1, 23) < 1$, *ns*, for hippocampus and $F(1, 26) < 1$, *ns*, for dACC. We next repeated this analysis with accuracy as the dependent variable. This revealed no significant correlation between Accuracy and Theta power changes in any of the three brain areas.

Together, these results show a significant positive correlation between the amount by which DLPFC theta power decreased as a function of memory load and the mean RT of a participant. Thus, the bigger the decrease with memory load was for a given participant during the maintenance period, the faster the response was of that participant (see Figure 10A; this was true for RTs in all loads). These results thus reveal that the extent of

DLPFC theta power decreases explain individual differences in RT in a WM task.

## DISCUSSION

The main aim of this study was to compare theta power changes as a function of memory load during WM maintenance between three brain areas: the DLPFC, the hippocampus, and the dACC. The reason for doing so is that these three areas have long been thought to be critical for WM (Bähner et al., 2015; Barbey, Koenigs, & Grafman, 2013; Lenartowicz & McIntosh, 2005), but it remains unclear how each of these areas contributes to information maintenance in WM. Although our study cannot claim to answer this question, the differences we identify here between these three brain areas indicate that DLPFC's contribution is different than those from other areas because it was the only area we investigated that exhibited prominent power decreases. We found that DLPFC broad band power decreased relative to baseline, and only for the theta band, power decreased proportionally to memory load stronger than this decrease was. Also, the extent of this power decrease was predictive of behavior on both a single-trial and subject-by-subject level. That is, people who were found to have a relatively bigger decrease in theta power were overall faster in accessing WM. In addition, we also found theta power changes in hippocampus and dACC. Strikingly, these were less pronounced and in the opposite direction compared with those in the DLPFC: In these areas, theta power increased relative to baseline and as a function of load. Note that the power modulations we revealed were selective to the theta band only when we consider effects of load (Figure 4). In contrast, the more general task versus baseline comparisons exhibited broadband effects (Figure 5). This finding allows the hypothesis that theta band power changes are specifically critical for WM maintenance.

Hippocampal theta has been extensively studied in both animals and humans, making its function relatively well understood (e.g., increases in theta power are associated with greater engagement and lead to better memory; see, e.g., Lin et al., 2017). In contrast, the properties of theta in neocortex are less understood, making it unclear whether patterns similar to hippocampal theta modulation would be expected. Additionally, some studies show that theta power recorded on the scalp is inversely correlated with fMRI BOLD changes (Michels et al., 2010; Scheeringa et al., 2008, 2009). Here, we found that the patterns of theta power modulation were of opposite sign in DLPFC versus dACC and hippocampus, arguing for a differential role of theta in these two areas.

The load-related theta power changes in DLPFC that we found resemble those observed in DLPFC using both fMRI BOLD as well as more direct measures of neural activity, but with opposite sign: BOLD or single-neuron studies reveal increases in activity as a function of memory load, whereas we here show a decrease in theta power as a function of memory load (Riley & Constantinidis, 2016; Veltman, Rombouts, & Dolan, 2003). One potential mechanism by which these differential effects can be explained is by considering the hypothesis that low-frequency oscillations in neocortex are an index of excitability, with higher power indicative of less excitability. Related to this, it has indeed been hypothesized (Lisman & Jensen, 2013) that neocortical theta oscillations might have a role similar to cortical alpha, which is thought to index cortical excitability. Thus, if we assume that theta power indexes cortical excitability in ways similar to alpha power (Lisman & Jensen, 2013) and if we assume that less excitability is less metabolically demanding, then our results are in agreement with the literature on BOLD fMRI studies of WM in DLPFC.

Overall, our results support a distinction between how the medial and lateral parts of pFC support WM maintenance. Medial pFC shows increases in theta power (both in scalp EEG and intracranial recordings) and decrease in fMRI BOLD activity as a function of load (Gusnard & Raichle, 2001). On the other hand, the fMRI BOLD signal increases in lateral parts of pFC during WM task performance, whereas the intracranial recordings described here as well as other existing studies (see Table 3) reveal decreases in theta power.

Several other intracranial studies considered changes of iEEG power during WM tasks (see Table 3 for summary). However, most of these focus on the task-related activity changes (compared with baseline activity) rather than prediction of behavior or load related changes (Meltzer et al., 2008; Raghavachari et al., 2001, 2006; Howard et al., 2003). An exception is the work of Meltzer et al. (2008), which compared the percentage of electrodes with positive or negative load-related power changes in patients performing a numerical Sternberg task between different regions of the brain. When comparing lateral (frontal, parietal) with medial (across entire medial wall) areas, they found that the percentage of electrodes with decreasing theta power as a function of load was larger in later compared with medial parts. Although this coarse analysis does not allow conclusions specific to DLPFC, dACC, or hippocampus, this pattern is nevertheless compatible with that which we found here.

We previously studied the same task at the single-neuron level in dACC and hippocampus (but not DLPFC, where no neurons were recorded; Kamiński et al., 2017). This previous work revealed that stimulus-selective neurons in the hippocampus maintained their activity throughout the maintenance period if their preferred stimulus was held in mind. The level of this persistent activity scaled inversely with load, with higher loads resulting in weaker persistent activity. In dACC, this previous study revealed non-stimulus-selective maintenance units that maintained their elevated level of activity throughout the maintenance period. Single-neuron activity was thus elevated throughout the maintenance period in both areas, but the selectivity of this activity was different between brain areas. Here,

**Table 3.** Summary of Theta Power Changes during Maintenance in Sternberg-like Tasks in Previously Published Human Intracranial Studies

| *Study* | *Localization of the Effect* | *Method* | *Task* | *Task Effect (vs. Baseline)* | *Load Effect* |
|---|---|---|---|---|---|
| Howard et al., 2003 | Temporal/frontal, occipital | iEEG | Verbal Sternberg | Mixed-effects, some channels increase, some decrease—inconclusive (according to the authors) | Not explored in theta (visible in gamma) |
| Raghavachari et al., 2001 | 74 electrodes of 247 (24 in the temporal lobe, 18 in the occipital lobe, 18 in the parietal/motor/premotor areas, and 14 in the frontal lobe) | iEEG | Verbal Sternberg | Mixed-effects, mostly increase but on subject showed decrease at some trials | Not explored |
| Raghavachari et al., 2006 | Occipital/ parietal (45/157), temporal (23/280), frontal (2/182) | Subdural and depths | Verbal Sternberg | Increase of power | Not explored |
| Axmacher et al., 2010 | Hippocampus | iEEG | Visual Sternberg | No data | No load-related power effects |
| Meltzer et al., 2008 | Midline and lateral part of pFC | iEEG | Numerical Sternberg | No data | Midline frontal sites: increase in theta/alpha<br>Lateral frontal sites: decrease in theta/alpha |
| van Vugt, Schulze-Bonhage, Litt, Brandt, & Kahana, 2010 | Prefrontal cortex and hippocampus | Subdural and depths | Sternberg with faces and letters | Not explored | Left lateral pFC—decrease for faces (40% of contacts), not letters (shown only in Figure 2)<br>Hippocampus—increase, right: 20% of contacts, left: 15% (shown in Figure 2 as well as in Table 2) |

we similarly found that power was changed relative to baseline throughout the baseline period and that such power changes scaled with load in different ways in different brain areas. It remains an open question how these single-neuron activity changes related to simultaneously recorded power changes and in particular how and whether the activity of single neurons in the human DLPFC is related to load during maintenance.

The theta power changes observed in our study in the DLPFC are different from those found in human EEG studies on FMT, which show that FMT power increases parametrically with memory load and/or the cognitive complexity of the task (Gärtner et al., 2015; Hsieh & Ranganath, 2014; Onton et al., 2005). FMT theta is recorded from electrodes placed over the frontal midline (Gärtner et al., 2015; Maurer et al., 2015; Hsieh & Ranganath, 2014; Anguera et al., 2013; Kamiński, Brzezicka, & Wróbel, 2011; Jensen & Tesche, 2002), with a source that is frequently localized in the anterior cingulate (Hsieh & Ranganath, 2014; Onton et al., 2005). Surprisingly, we did not find load-related theta power changes in dACC that were similar to those observed with FMT. Although we found that theta power increased during maintenance relative to baseline, the extent of this increase was not significantly related to memory load. One possibility is that parts of FMT are in fact volume-conducted hippocampal theta. In addition, it is not known what the contribution of DLPFC is to FMT. Simultaneous scalp EEG (FMT) and intracranial dACC, hippocampal, and DLPFC recordings will be required to directly investigate this potential discrepancy, in particular in light of recent work that indicates that local field potential and EEG power can be disassociated in some instances (Musall, von Pföstl, Rauch, Logothetis, & Whittingstall, 2014).

Our results are also of relevance to a recently proposed model on the interplay between hippocampus and neocortex during episodic memory formation (Parish, Hanslmayr, & Bowman, 2018). This model proposes that lower frequency oscillations (alpha in their case) have different roles in the hippocampus and cortex (Parish et al., 2018). The reasoning for this rests on two assumptions. First, neurons in neocortex need to "break out" of an ongoing oscillation to represent a stimulus, which is achieved by desynchronization. Second, firing of hippocampal neurons in synchrony with ongoing theta oscillations facilitates formation of memories (i.e., theta synchronizes). Accordingly, successful memory formation is marked by both reduced neocortical alpha and increased hippocampal theta. Although originally proposed for episodic memory, our data suggest that this mode of operation might also be valid for WM, with theta serving two different roles—desynchronizing activity of neurons in neocortex (DLPFC) and synchronizing in hippocampus during WM maintenance. A key caveat is, however, that here we did not quantify synchronization. Rather, we measured only power changes, which might be due to changes in synchronization but can also result from other type of activity changes. Answering this question conclusively will require quantifying synchrony between pairs of neurons recorded in DLPFC, which is data that we do not have access to here.

An important question that our results raise is how power decreases in a given area can be functionally beneficial (as ours were, as demonstrated by the correlation with behavior). With respect to theta, this question is little studied, because most of the literature so far focused on power increases and their functional role. One hypothesis is that neurons that code for particular stimuli form small ensembles and synchronize with each other at different (mostly higher than theta) frequencies, resulting in decreased theta power for higher loads. Another hypothesis is that there are several independent local theta generators (i.e., here one for hippocampus, one for DLPFC) that change differently as a function of load (Raghavachari et al., 2006). Note that, in contrast to theta, beta power reductions and the resulting desynchronization are prominent phenomena in the motor system that are well understood and which are necessary for properly releasing a motor movement (Crowell et al., 2012). So a third hypothesis is that in DLPFC theta acts akin to beta in the motor cortex.

What function does a WM theta power decrease in the DLPFC index? WM involves several theoretical constructs (see, e.g., Conway, Jarrold, Kane, Miyake, & Towse, 2007), including one related to cognitive control and another related to storage itself. Our task only concerns storage, but no active manipulations during maintenance. In addition, we observe prominent load-related changes in neural activity. For this reason, we hypothesize that the theta power decrease we found in DLPFC is a reflection of the storage component of WM. A key question that remains to be answered is what the relationship is between these power decreases and the activity of individual neurons in DLPFC. One hypothesis is that, as a result of reduced power, synchrony between pairs of neurons in DLPFC would decrease, thereby allowing more independent storage of different items. Single-neuron recordings in DLPFC will be required to answer this question. Of relevance, recent work (de Vries, van Driel, Karacaoglu, & Olivers, 2018) suggests that frontal areas might use low-frequency theta to drive changes in more posterior areas, and thus, the role of pFC might be crucial for storage only indirectly, because the storage as such takes place elsewhere.

Our results seem also to be contradictory to the "theta gating" hypothesis (Raghavachari et al., 2001), which proposes that the amplitude of theta oscillations increases at the start of a cognitive task (e.g., Sternberg task), then continues to be elevated through all phases of the trial, including the delay period, and decreases sharply at the end of the maintaining period. However, this effect is not apparent on all electrodes analyzed (Raghavachari et al., 2001). Rather, its presence is conditional on where an electrode was placed, with some electrodes showing the opposite pattern (Raghavachari et al., 2001). This is compatible with our observation, which shows that the

pattern of change depends on where in the cortex theta is recorded from. It might be possible that neocortical areas are more likely to show theta decreases compared with allocortex (hippocampus, dACC). Such thinking is supported by some animal studies. For example, studies utilizing macaques performing a visual WM task (Kornblith, Buschman, & Miller, 2016) have revealed load-related decrease in low-frequency power.

Is the activity in DLPFC that we measure here related to preparatory motor activity, thereby explaining the ability of theta power in DLPFC to predict response speed? To exclude this possibility, we only included data during the maintenance period, excluding data from the probe period in our analysis. In addition, the maintenance period length was unpredictable, making it impossible for a participant to know when the probe image was displayed. For this reason, we do not believe that the theta power reduction we observed in DLPFC is a reflection of motor preparation.

Our results show that task- and load-related theta power changes in the DLPFC predict an individual person's accuracy and speed during a WM task. Note, however, that due to the limited size of our participant pool (13 participants), the statistical power to explain individual differences in this data set is limited, and larger studies are needed to confirm these putative individual differences. We found this relationship on two levels: intra- and interindividual. We saw that trials characterized by a bigger drop in theta power during maintenance compared with the baseline were more likely to end with the patient producing a correct response, with a faster RT. We also found that participants exhibiting a greater amount of theta decrease in the DLPFC had faster RTs. These results support the view that DLPFC theta power changes explain individual differences in RT in a WM task. WM ability varies greatly between individuals (Shipstead et al., 2016; Unsworth & Engle, 2006, 2007), with important consequences for a person's overall cognitive function. It is thus important to discover features of WM that differ between individuals. Here, we found such a relationship in DLPFC. This extends previous work using scalp EEG, in which we found a similar relationship for FMT (Zakrzewska & Brzezicka, 2014). Together, these data indicate that theta power in DLPFC is a metric that may help explain individual differences in WM and may be used as a neurophysiological indicator of WM efficiency.

Reprint requests should be sent to Ueli Rutishauser, Division of Biology and Biological Engineering, California Institute of Technology, 1200 E. California Blvd., Pasadena, CA 91125, or via e-mail: urut@caltech.edu.

## REFERENCES

Altamura, M., Elvevåg, B., Blasi, G., Bertolino, A., Callicott, J. H., Weinberger, D. R., et al. (2007). Dissociating the effects of Sternberg working memory demands in prefrontal cortex. *Psychiatry Research: Neuroimaging*, *154*, 103–114.

Anguera, J. A., Boccanfuso, J., Rintoul, J. L., Al-Hashimi, O., Faraji, F., Janowich, J., et al. (2013). Video game training enhances cognitive control in older adults. *Nature*, *501*, 97–101.

Asada, H., Fukuda, Y., Tsunoda, S., Yamaguchi, M., & Tonoike, M. (1999). Frontal midline theta rhythms reflect alternative activation of prefrontal cortex and anterior cingulate cortex in humans. *Neuroscience Letters*, *274*, 29–32.

Avants, B. B., Duda, J. T., Kim, J., Zhang, H., Pluta, J., Gee, J. C., et al. (2008). Multivariate analysis of structural and diffusion imaging in traumatic brain injury. *Academic Radiology*, *15*, 1360–1375.

Axmacher, N., Henseler, M. M., Jensen, O., Weinreich, I., Elger, C. E., & Fell, J. (2010). Cross-frequency coupling supports multi-item working memory in the human hippocampus. *Proceedings of the National Academy of Sciences, U.S.A.*, *107*, 3228–3233.

Baddeley, A. (2010). Working memory. *Current Biology*, *20*, R136–R140.

Bagherzadeh, Y., Khorrami, A., Zarrindast, M. R., Shariat, S. V., & Pantazis, D. (2016). Repetitive transcranial magnetic stimulation of the dorsolateral prefrontal cortex enhances working memory. *Experimental Brain Research*, *234*, 1807–1818.

Bähner, F., Demanuele, C., Schweiger, J., Gerchen, M. F., Zamoscik, V., Ueltzhöffer, K., et al. (2015). Hippocampal-dorsolateral prefrontal coupling as a species-conserved cognitive mechanism: A human translational imaging study. *Neuropsychopharmacology*, *40*, 1674–1681.

Barbey, A. K., Koenigs, M., & Grafman, J. (2013). Dorsolateral prefrontal contributions to human working memory. *Cortex*, *49*, 1195–1205.

Conway, A. R. A., Jarrold, C., Kane, M. J., Miyake, A., & Towse, J. N. (2007). Variation in working memory: An introduction. In A. R. A. Conway, C. Jarrold, M. J. Kane, A. Miyake, & J. N. Towse (Eds.), *Variation in working memory* (pp. 3–17). New York: Oxford University Press.

Crowell, A. L., Ryapolova-Webb, E. S., Ostrem, J. L., Galifianakis, N. B., Shimamoto, S., Lim, D. A., et al. (2012). Oscillations in sensorimotor cortex in movement disorders: An electrocorticography study. *Brain*, *135*, 615–630.

Curtis, C. E., & D'Esposito, M. (2003). Persistent activity in the prefrontal cortex during working memory. *Trends in Cognitive Sciences*, *7*, 415–423.

Delorme, A., & Makeig, S. (2004). EEGLAB: An open source toolbox for analysis of single-trial EEG dynamics including independent component analysis. *Journal of Neuroscience Methods*, *134*, 9–21.

de Vries, I. E. J., van Driel, J., Karacaoglu, M., & Olivers, C. N. L. (2018). Priority switches in visual working memory are supported by frontal delta and posterior alpha interactions. *Cerebral Cortex*, *28*, 4090–4104.

Finn, A. S., Sheridan, M. A., Kam, C. L. H., Hinshaw, S., & D'Esposito, M. (2010). Longitudinal evidence for functional specialization of the neural circuit supporting working memory in the human brain. *Journal of Neuroscience*, *30*, 11062–11067.

Funahashi, S. (2017). Working memory in the prefrontal cortex. *Brain Sciences*, *7*, 49.

Fuster, J. M. (1973). Unit activity in prefrontal cortex during delayed-response performance: Neuronal correlates of transient memory. *Journal of Neurophysiology*, *36*, 61–78.

Fuster, J. M., & Alexander, G. E. (1971). Neuron activity related to short-term memory. *Science*, *173*, 652–654.

Gärtner, M., Grimm, S., & Bajbouj, M. (2015). Frontal midline theta oscillations during mental arithmetic: Effects of stress. *Frontiers in Behavioral Neuroscience*, *9*, 96.

Goldman-Rakic, P. S. (1995). Cellular basis of working memory. *Neuron*, *14*, 477–485.

Gusnard, D. A., & Raichle, M. E. (2001). Searching for a baseline: Functional imaging and the resting human brain. *Nature Reviews Neuroscience*, *2*, 685–694.
Helfrich, R. F., & Knight, R. T. (2016). Oscillatory dynamics of prefrontal cognitive control. *Trends in Cognitive Sciences*, *20*, 916–930.
Howard, M. W., Rizzuto, D. S., Caplan, J. B., Madsen, J. R., Lisman, J., Aschenbrenner-Scheibe, R., et al. (2003). Gamma oscillations correlate with working memory load in humans. *Cerebral Cortex*, *13*, 1369–1374.
Hsieh, L.-T., & Ranganath, C. (2014). Frontal midline theta oscillations during working memory maintenance and episodic encoding and retrieval. *Neuroimage*, *85*, 721–729.
Jansma, J. M., Ramsey, N. F., de Zwart, J. A., van Gelderen, P., & Duyn, J. H. (2007). fMRI study of effort and information processing in a working memory task. *Human Brain Mapping*, *28*, 431–440.
Jensen, O., & Tesche, C. D. (2002). Frontal theta activity in humans increases with memory load in a working memory task. *European Journal of Neuroscience*, *15*, 1395–1399.
Kamiński, J., Brzezicka, A., & Wróbel, A. (2011). Short-term memory capacity ($7 \pm 2$) predicted by theta to gamma cycle length ratio. *Neurobiology of Learning and Memory*, *95*, 19–23.
Kamiński, J., Sullivan, S., Chung, J. M., Ross, I. B., Mamelak, A. N., & Rutishauser, U. (2017). Persistently active neurons in human medial frontal and medial temporal lobe support working memory. *Nature Neuroscience*, *20*, 590–601.
Kornblith, S., Buschman, T. J., & Miller, E. K. (2016). Stimulus load and oscillatory activity in higher cortex. *Cerebral Cortex*, *26*, 3772–3784.
Lara, A. H., & Wallis, J. D. (2015). The role of prefrontal cortex in working memory: A mini review. *Frontiers in Systems Neuroscience*, *9*, 173.
Lee, H., Simpson, G. V., Logothetis, N. K., & Rainer, G. (2005). Phase locking of single neuron activity to theta oscillations during working memory in monkey extrastriate visual cortex. *Neuron*, *45*, 147–156.
Lega, B. C., Jacobs, J., & Kahana, M. (2012). Human hippocampal theta oscillations and the formation of episodic memories. *Hippocampus*, *22*, 748–761.
Lenartowicz, A., & McIntosh, A. R. (2005). The role of anterior cingulate cortex in working memory is shaped by functional connectivity. *Journal of Cognitive Neuroscience*, *17*, 1026–1042.
Lin, J.-J., Rugg, M. D., Das, S., Stein, J., Rizzuto, D. S., Kahana, M. J., et al. (2017). Theta band power increases in the posterior hippocampus predict successful episodic memory encoding in humans. *Hippocampus*, *27*, 1040–1053.
Lisman, J. E., & Jensen, O. (2013). The theta-gamma neural code. *Neuron*, *77*, 1002–1016.
Manoach, D. S., Schlaug, G., Siewert, B., Darby, D. G., Bly, B. M., Benfield, A., et al. (1997). Prefrontal cortex fMRI signal changes are correlated with working memory load. *NeuroReport*, *8*, 545–549.
Maris, E., & Oostenveld, R. (2007). Nonparametric statistical testing of EEG- and MEG-data. *Journal of Neuroscience Methods*, *164*, 177–190.
Maurer, U., Brem, S., Liechti, M., Maurizio, S., Michels, L., & Brandeis, D. (2015). Frontal midline theta reflects individual task performance in a working memory task. *Brain Topography*, *28*, 127–134.
Meltzer, J. A., Negishi, M., Mayes, L. C., & Constable, R. T. (2007). Individual differences in EEG theta and alpha dynamics during working memory correlate with fMRI responses across subjects. *Clinical Neurophysiology*, *118*, 2419–2436.
Meltzer, J. A., Zaveri, H. P., Goncharova, I. I., Distasio, M. M., Papademetris, X., Spencer, S. S., et al. (2008). Effects of working memory load on oscillatory power in human intracranial EEG. *Cerebral Cortex*, *18*, 1843–1855.
Michels, L., Bucher, K., Lüchinger, R., Klaver, P., Martin, E., Jeanmonod, D., et al. (2010). Simultaneous EEG-fMRI during a working memory task: Modulations in low and high frequency bands. *PLoS One*, *5*, e10298.
Minxha, J., Mamelak, A. N., & Rutishauser, U. (2018). Surgical and electrophysiological techniques for single-neuron recordings in human epilepsy patients. In R. Sillitoe (Ed.), *Extracellular recording approaches* (Vol. *134*, pp. 267–293). New York: Humana Press.
Minxha, J., Mosher, C., Morrow, J. K., Mamelak, A. N., Adolphs, R., Gothard, K. M., et al. (2017). Fixations gate species-specific responses to free viewing of faces in the human and macaque amygdala. *Cell Reports*, *18*, 878–891.
Mitchell, D. J., McNaughton, N., Flanagan, D., & Kirk, I. J. (2008). Frontal-midline theta from the perspective of hippocampal "theta." *Progress in Neurobiology*, *86*, 156–185.
Morgan, H. M., Jackson, M. C., van Koningsbruggen, M. G., Shapiro, K. L., & Linden, D. E. J. (2013). Frontal and parietal theta burst TMS impairs working memory for visual-spatial conjunctions. *Brain Stimulation*, *6*, 122–129.
Musall, S., von Pföstl, V., Rauch, A., Logothetis, N. K., & Whittingstall, K. (2014). Effects of neural synchrony on surface EEG. *Cerebral Cortex*, *24*, 1045–1053.
Mylius, V., Ayache, S. S., Ahdab, R., Farhat, W. H., Zouari, H. G., Belke, M., et al. (2013). Definition of DLPFC and M1 according to anatomical landmarks for navigated brain stimulation: Inter-rater reliability, accuracy, and influence of gender and age. *Neuroimage*, *78*, 224–232.
Nouwens, S., Groen, M. A., & Verhoeven, L. (2017). How working memory relates to children's reading comprehension: The importance of domain-specificity in storage and processing. *Reading and Writing*, *30*, 105–120.
Onton, J., Delorme, A., & Makeig, S. (2005). Frontal midline EEG dynamics during working memory. *Neuroimage*, *27*, 341–356.
Parish, G., Hanslmayr, S., & Bowman, H. (2018). The Sync/deSync model: How a synchronized hippocampus and a desynchronized neocortex code memories. *Journal of Neuroscience*, *38*, 3428–3440.
Raghavachari, S., Kahana, M. J., Rizzuto, D. S., Caplan, J. B., Kirschen, M. P., Bourgeois, B., et al. (2001). Gating of human theta oscillations by a working memory task. *Journal of Neuroscience*, *21*, 3175–3183.
Raghavachari, S., Lisman, J. E., Tully, M., Madsen, J. R., Bromfield, E. B., & Kahana, M. J. (2006). Theta oscillations in human cortex during a working-memory task: Evidence for local generators. *Journal of Neurophysiology*, *95*, 1630–1638.
Rajkowska, G., & Goldman-Rakic, P. S. (1995). Cytoarchitectonic definition of prefrontal areas in the normal human cortex: I. Remapping of areas 9 and 46 using quantitative criteria. *Cerebral Cortex*, *5*, 307–322.
Reuter, M., Rosas, H. D., & Fischl, B. (2010). Highly accurate inverse consistent registration: A robust approach. *Neuroimage*, *53*, 1181–1196.
Riley, M. R., & Constantinidis, C. (2016). Role of prefrontal persistent activity in working memory. *Frontiers in Systems Neuroscience*, *9*, 181.
Rottschy, C., Langner, R., Dogan, I., Reetz, K., Laird, A. R., Schulz, J. B., et al. (2012). Modelling neural correlates of working memory: A coordinate-based meta-analysis. *Neuroimage*, *60*, 830–846.
Roux, F., & Uhlhaas, P. J. (2014). Working memory and neural oscillations: Alpha-gamma versus theta-gamma codes for distinct WM information? *Trends in Cognitive Sciences*, *18*, 16–25.

Scheeringa, R., Bastiaansen, M. C. M., Petersson, K. M., Oostenveld, R., Norris, D. G., & Hagoort, P. (2008). Frontal theta EEG activity correlates negatively with the default mode network in resting state. *International Journal of Psychophysiology*, *67*, 242–251.

Scheeringa, R., Petersson, K. M., Oostenveld, R., Norris, D. G., Hagoort, P., & Bastiaansen, M. C. M. (2009). Trial-by-trial coupling between EEG and BOLD identifies networks related to alpha and theta EEG power increases during working memory maintenance. *Neuroimage*, *44*, 1224–1238.

Schicktanz, N., Fastenrath, M., Milnik, A., Spalek, K., Auschra, B., Nyffeler, T., et al. (2015). Continuous theta burst stimulation over the left dorsolateral prefrontal cortex decreases medium load working memory performance in healthy humans. *PLoS One*, *10*, e0120640.

Ségonne, F., Dale, A. M., Busa, E., Glessner, M., Salat, D., Hahn, H. K., et al. (2004). A hybrid approach to the skull stripping problem in MRI. *Neuroimage*, *22*, 1060–1075.

Shipstead, Z., Harrison, T. L., & Engle, R. W. (2016). Working memory capacity and fluid intelligence: Maintenance and disengagement. *Perspectives on Psychological Science*, *11*, 771–799.

Spellman, T., Rigotti, M., Ahmari, S. E., Fusi, S., Gogos, J. A., & Gordon, J. A. (2015). Hippocampal–prefrontal input supports spatial encoding in working memory. *Nature*, *522*, 309–314.

Sternberg, S. (1966). High speed scanning in human memory. *Science*, *153*, 652–654.

Tesche, C. D., & Karhu, J. (2000). Theta oscillations index human hippocampal activation during a working memory task. *Proceedings of the National Academy of Sciences, U.S.A.*, *97*, 919–924.

The MathWorks. (2015). MATLAB 2015a. Natick, MA.

Tsujimoto, T., Shimazu, H., Isomura, Y., & Sasaki, K. (2010). Theta oscillations in primate prefrontal and anterior cingulate cortices in forewarned reaction time tasks. *Journal of Neurophysiology*, *103*, 827–843.

Tyszka, J. M., & Pauli, W. M. (2016). In vivo delineation of subdivisions of the human amygdaloid complex in a high-resolution group template. *Human Brain Mapping*, *37*, 3979–3998.

Unsworth, N., & Engle, R. W. (2006). Simple and complex memory spans and their relation to fluid abilities: Evidence from list-length effects. *Journal of Memory and Language*, *54*, 68–80.

Unsworth, N., & Engle, R. W. (2007). The nature of individual differences in working memory capacity: Active maintenance in primary memory and controlled search from secondary memory. *Psychological Review*, *114*, 104–132.

van Vugt, M. K., Schulze-Bonhage, A., Litt, B., Brandt, A., & Kahana, M. J. (2010). Hippocampal gamma oscillations increase with memory load. *Journal of Neuroscience*, *30*, 2694–2699.

Veltman, D. J., Rombouts, S. A. R. B., & Dolan, R. J. (2003). Maintenance versus manipulation in verbal working memory revisited: An fMRI study. *Neuroimage*, *18*, 247–256.

Wang, X.-J. (2010). Neurophysiological and computational principles of cortical rhythms in cognition. *Physiological Reviews*, *90*, 1195–1268.

Wiley, J., & Jarosz, A. F. (2012). How working memory capacity affects problem solving. In B. H. Ross (Ed.), *The psychology of learning and motivation* (Vol. *56*, pp. 185–227). San Diego: Academic Press.

Wisniewski, M. G., Thompson, E. R., Iyer, N., Estepp, J. R., Goder-Reiser, M. N., & Sullivan, S. C. (2015). Frontal midline θ power as an index of listening effort. *NeuroReport*, *26*, 94–99.

Womelsdorf, T., Johnston, K., Vinck, M., & Everling, S. (2010). Theta-activity in anterior cingulate cortex predicts task rules and their adjustments following errors. *Proceedings of the National Academy of Sciences, U.S.A.*, *107*, 5248–5253.

Yoon, T., Okada, J., Jung, M. W., & Kim, J. J. (2008). Prefrontal cortex and hippocampus subserve different components of working memory in rats. *Learning & Memory*, *15*, 97–105.

Zakrzewska, M. Z., & Brzezicka, A. (2014). Working memory capacity as a moderator of load-related frontal midline theta variability in Sternberg task. *Frontiers in Human Neuroscience*, *8*, 399.